Chinese Journal of Polymer Science Vol. 33, No. 7, (2015), 1058–1068

Chinese Journal of Polymer Science

Enhancement of Mechanical Properties of Natural Rubber with Maleic Anhydride Grafted Liquid Polybutadiene Functionalized Graphene Oxide*

Long-mei Wu[a], Shuang-quan Liao[b**], Sheng-jun Zhang[b], Xiao-ying Bai[b] and Xue Hou[b]
[a] *College of Agriculture, Hainan University, Haikou 570228, China*
[b] *College of Materials and Chemical Engineering, Hainan University, Haikou 570228, China*

Abstract An effective procedure has been developed to synthesize the functionalized graphene oxide grafted by maleic anhydride grafted liquid polybutadiene (MLPB-GO). Fourier transform spectroscopy and X-ray photoelectron spectroscopy indicate the successful functionalization of GO. The NR/MLPB-GO composites were then prepared by the co-coagulation process. The results show that the mechanical properties of NR/MLPB-GO composites are obviously superior to those of NR/GO composites and neat NR. Compared with neat NR, the tensile strength, modulus at 300% strain and tear strength of NR composite containing 2.12 phr MLPB-GO are significantly increased by 40.5%, 109.1% and 85.0%, respectively. Dynamic mechanical analysis results show that 84% increase in storage modulus and 2.9 K enhancement in the glass transition temperature of the composite have been achieved with the incorporation of 2.12 phr MLPB-GO into NR. The good dispersion of GO and the strong interface interaction in the composites are responsible for the unprecedented reinforcing efficiency of MLPB-GO towards NR.

Keywords: Enhancement; Maleic anhydride-grafted liquid polybutadiene; Graphene oxide; Composites; Mechanical properties.

INTRODUCTION

Elastomers are usually reinforced with nano-scale fillers to get substantial improvements in overall performances, meeting the demands in the specific properties and practical applications. Up to date, nano-scale reinforcing fillers have received considerable attention from elastomer scientists due to their nanometer effect and high specific surface area, which can achieve the required mechanical properties at low filler loadings[1, 2]. Recently, graphene oxide (GO), as a nano-scale carbon material with unique physical properties[3–5], has been demonstrated to be a promising reinforcing filler for polymer composites because of extremely high specific surface area, high modulus, water solubility and versatile surface characteristics.

To maximize the reinforcing efficiency of GO in polymer composites, the issues of the interfacial adhesion between GO-matrix and the dispersion state of GO should be addressed. It is well known that GO sheets bear various oxygen-containing groups, including epoxides, hydroxyls and carboxyls on the sheets, which impart the miscibility between GO and some polar polymers. Recently, GO has been integrated into polar polymers such as carboxylated acrylonitrile butadiene rubber (XNBR)[6], poly(vinyl alcohol)[7] and cellulose[8] *via* solution mixing. The interfacial interaction between these polymers and GO has been substantiated to be hydrogen bonding[6, 9, 10].

* This work was financially supported by the National Natural Science Foundation of China (No. 51363006), Science and Technology innovation key project of Hainan province (No. ZDXM20120090), National Science and Technology support project (No. 2013BAF08B02).
** Corresponding author: Shuang-quan Liao (廖双泉), E-mail: shqliao@263.net
Received November 29, 2014; Revised February 25, 2015; Accepted March 14, 2015
doi: 10.1007/s10118-015-1652-9

Nevertheless, the hydrogen bonding interaction is not strong enough to suppress the aggregation of GO sheets during the evaporation of solvent and efficiently transfer the load from the matrix to GO sheets under stress. In order to improve the miscibility between GO and other polymer matrices, many methods have been developed, including surface-initiated polymerization[11], *in situ* miniemulsion polymerization[12] and covalent functionalization of GO[13–15]. Nowadays, covalent functionalization is a very efficient and simple approach to modify the GO sheets[16–19]. For example, Pham *et al*. have proposed a new modification technique for the preparation of a water-dispersible polyglycerol-grafted GO[20]. Avinash *et al*. have demonstrated Friedel-Crafts acylation of GO with ferrocene[21]. And Stankovich *et al*. used a series of isocyanate compounds in the surface modification of GO using condensation reaction[22]. Among these modification method, the functional groups on the GO sheets could serve as reaction sites and further promote derivatization reactions, greatly improving the compatibility between the GO and polymer matrices. Although covalent functionalization is envisaged as efficient way to improve GO dispersion in a polar polymer matrix and enhance the interfacial adhesion between them, it is not efficient to afford strong interface interaction between the non-polar polymers and GO. Thus, simple and effective approaches to improve the interfacial interaction in non-polar polymer/GO composites are worth to exploring.

Maleic anhydride grafted liquid polybutadiene (MLPB), as a product of polybutadiene with low molecular weight modified by maleic anhydride, can be used as a modifier or a coupling agent for organic-inorgonic fillers and polymers[23, 24]. The MLPB molecule owns flexible long-chain and anhydride groups. The functionalization can proceed through a ring-opening reaction between the carboxyl groups of fillers and the anhydride groups of MLPB by the action of nucleophilic reagents. It is noteworthy that MLPB with vinyls is highly unsaturated. The unsaturated double bond provides the active crosslink point during the vulcanization, forming the complex crosslinked network. Therefore, a remarkable improvement of interfacial adhesion between fillers and rubber matrices can be achieved by incorporating fillers functionalized by MLPB.

In this work, MLPB grafted GO sheets (MLPB-GO) were prepared by covalent functionalization, then NR/MLPB-GO composites were fabricated by the co-coagulation process. The covalent functionalization was fully verified for MLPB-GO. Also, the reinforcing effects of MLPB-GO on the morphology and mechanical performances of NR composites were investigated.

EXPERIMENTAL

Materials

Natural graphite powder was purchased from Qingdao Xinghua Graphite Product Co., Ltd. Hydrochloric acid (HCl, 36%), sulfuric acid (H_2SO_4, 98%), potassium permanganate ($KMnO_4$), sodium nitrite ($NaNO_3$), hydrogen peroxide (H_2O_2, 30%), sodium dodecyl sulfonate (SDS), acetone, *p*-toluenesulfonic acid (*p*-TSA), and calcium chloride were obtained from Guangzhou Chemical Reagent Factory. Maleic anhydride-grafted liquid polybutadiene (MLPB) terminated by *p*-xyene (M_n = 2200), was received from Guangzhou Qingsheng Rubber Technology Co., Ltd. All the reagents were of analytical grade and were used as received without further purification.

Natural rubber latex (NRL) was supplied by Guangzhou Rubber Institute. Zinc oxide (ZnO), stearic acid, *N*-cyclohexylbenzothiazole-2-sulphenamide (CZ), 2,2′-dibenzothiazole disulfide (DM), 2-mercaptobenzimidazole (MB) and sulfur were purchased from Guangzhou Longsun Technology Co., Ltd. All the rubber ingredients were industrial grade and used as received.

Samples Preparation

Graphite oxide was synthesized from natural graphite powder by a modified Hummers method[25]. Typically, 3 g of natural graphite powder and 1.5 g of $NaNO_3$ were added into 120 mL of concentrated H_2SO_4, and then 12 g of $KMnO_4$ was slowly added to the mixture over an ice-water bath. After reaction with 2 h, the reaction mixture was stirred at 35 °C for 6 h, further diluted by 200 mL of deionized water. Then the mixture was kept reaction at 98 °C and maintained for 2 h, followed by adding 600 mL of water and 30% H_2O_2 until the mixture turned into

orange/gold in color. Afterwards, the products were filtered and repeatedly washed with 5% HCl and water. Finally, graphite oxide (yellow-brown solid) was obtained after dry in a vacuum oven at 60 °C for 12 h.

The grafting processes of MLPB onto GO sheets are shown in Scheme 1. Firstly, 100 mg of graphite oxide was dispersed in 250 mL of acetone with sonication for 1 h. The resulted suspension was centrifugated at 8000 r·min^{-1} for 0.5 h, followed by adding 100 mg of SDS. The homogeneous GO suspension was obtained. The suspension was then mixed with 300 mg of MLPB and 200 mg of *p*-TSA, and vigorously stirred at 70 °C for 12 h to obtain MLPB-GO. It was found that acetone is a most effective solvent to purify MLPB-GO, and the MLPB/acetone solution exhibits a brownish yellow color. Thus, in order to wash out the unreacted MLPB, the obtained product (MLPB-GO) was repeatedly washed in acetone by sonication and centrifugation. By centrifugation, the supernatant was actually colorless, and the deposit in the bottom was dispersed in acetone by sonication, exhibited the pale yellow. The colorless supernatant and the unchanged pale yellow solution all can prove that the residual and unreacted MLPB was clearly removed. To quantify the concentration of MLPB-GO/acetone suspension, three samplings of 5 mL of MLPB-GO/acetone were dried at 100 °C for 12 h to remove water and acetone. The concentration of MLPB-GO/acetone was obtained by taking the average value of the three samplings.

A designed amount of MLPB-GO suspension was added into the NR latex (solid content of 60 g) under vigorous stirring. Calcium chloride solution (3 wt%) as the flocculant was used for the co-coagulation. The resulted compounds were cut into small pieces and repeatedly washed with deionized water several times, and then dried at 60 °C for 12 h. The recipe for composites is given as follows: NR, 100 phr; ZnO, 5 phr; stearic acid, 2 phr; CZ, 1.5 phr; DM, 0.5 phr; MB, 1 phr; sulfur, 1.5 phr; MLPB-GO, variable. NR was mixed with the rubber ingredients on a conventional two-roll mill. And curing was carried out at 143 °C for the optimum curing time after placing at room temperature for 12 h. For comparison, an NR/GO composite was also prepared by the identical procedure. These vulcanizates are abbreviated as "MLPB-GO-*x*" or "GO-*x*" below. The unknown number *x* denotes MLPB-GO loading (phr) or GO loading (phr) in the composites.

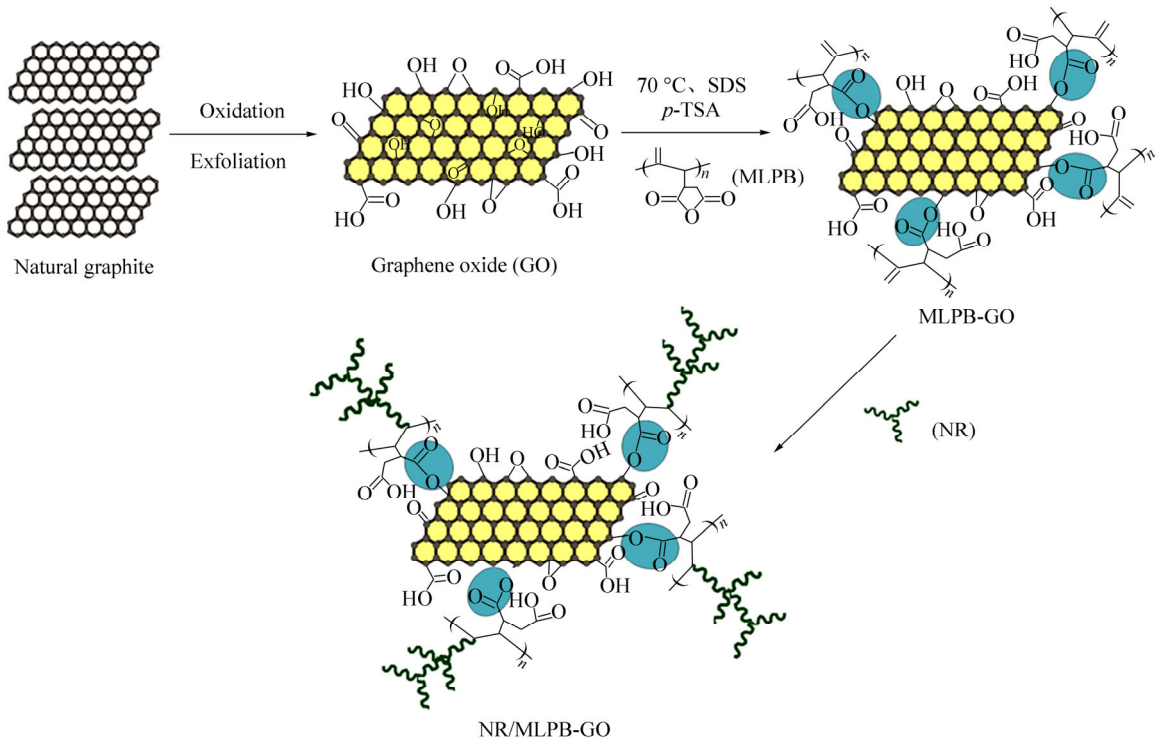

Scheme 1 The preparation of GO, MLPB-GO and NR/MLPB-GO composites

Testing

Fourier transform infrared spectroscopy (FTIR) spectra were collected on a Bruker VERTEX70 FTIR spectrometer. All the spectra were obtained at a resolution of 4 cm^{-1} in the wavenumber range of 400–4000 cm^{-1}. X-ray diffraction (XRD) analyses were carried out using a Bruker D8 Advance X-ray diffractometer with Cu Kα radiation (λ = 0.1542 nm), and the goniometer scanned diffracted X-rays at a scan speed of 0.15 (°)·s^{-1}. Thermogravimetric analysis (TGA) was collected on a Netzsch TG209F1 apparatus with a heating rate of 10 K·min^{-1} under nitrogen atmosphere. X-ray photoelectron spectrometer (XPS) analysis was carried out on a Kratos Axis Ultra DLD with Al Kα radiation (1486.6 eV) for investigating the surface compositions of GO and MLPB-GO. The morphology and composition of the synthetic composites were examined by field emission scanning electron microscopy (FESEM, NOVA NANOSEM 430) and high resolution transmission electron microscopy (HRTEM, JEOL2100). The vulcanization characteristics of the composites were obtained by a UR-2030SD Foam Pressure Rheometer. The mechanical properties were evaluated using a universal testing machine (U-CAN UT-2060, Taiwan) with a cross-head rate of 500 mm·min^{-1} at room temperature. The measurements of crosslink density and swell ratio were carried out by equilibrium swelling method as reported previously[26]. Dynamic mechanical analysis (DMA) was performed using a DMA242C instrument and all tests were conducted at 1 Hz from –120 °C to 80 °C by using a tensile mode. The heating rate was set at 3 K·min^{-1}.

RESULTS AND DISCUSSION

Structural Characterization of MLPB-GO

A schematic for the preparation of the MLPB-GO is illustrated in Scheme 1. The MLPB-GO was prepared by grafting MLPB onto GO sheets. Using *p*-TSA as a catalyst, the esterification reaction could occur between anhydride groups of MLPB and the hydroxyl groups of GO sheets. The graft modification of GO is verified by FTIR, as demonstrated in Fig. 1(a). As for GO, the spectrum presents the absorption peaks at 1043 cm^{-1} (C—O stretching vibrations), 1226 cm^{-1} (C—OH stretching vibrations), 1398 cm^{-1} (O—H deformation of the C—OH groups) and 1727 cm^{-1} (C=O stretching vibrations of the —COOH groups). These oxygen-containing groups were introduced into the graphite sheets during the oxidization process. And for MLPB, the peaks located at 1865 cm^{-1}, 1785 cm^{-1} were assigned to anhydride group in MLPB molecule. In the spectra of MLPB-GO, the broad peak ranging from 3100 cm^{-1} to 2800 cm^{-1} is ascribed to the $-CH_2-$ and $-CH_3$ stretching vibrations of the MLPB component, and the characteristic absorption at 1630 cm^{-1} is attributed to the stretching vibration of the C=C of the MLPB molecules and unoxidized graphitic domains. It is worth noting that the peaks attributed to anhydride group of MLPB disappeared after functionalization, and the peak at 1710 cm^{-1} corresponding to C=O stretching vibrations of the —COOH groups became shaper in comparison with GO. Such changes indicate the successful grafting of MLPB onto the GO sheets.

TGA was further used to investigate the graft modification of GO, as demonstrated in Fig. 1(b). In the TGA curve of GO, it starts to present some mass loss at about 100 °C and rapidly decomposes at about 200 °C, which can be attributed to the pyrolysis of thermally unstable oxygen containing groups, such as —OH and —COOH[27]. For the MLPB, the weight loss in the range of 300–500 °C is due to the decomposition of the MLPB backbone and the weight loss is nearly 100% at 800 °C. By grafting MLPB onto GO sheets, the thermal stability of GO can be effectively enhanced, with the maximum mass loss temperature increasing from 200 °C to 390 °C. The significant improvement in thermal stability is attributed to the MLPB macromolecules grafted onto the GO sheets, which delays the escape of thermally unstable oxygen containing groups. Considering that the weight loss is due to the removal of MLPB and oxygen containing groups, the residual weight implies that the grafted MLPB content is about 30 wt%.

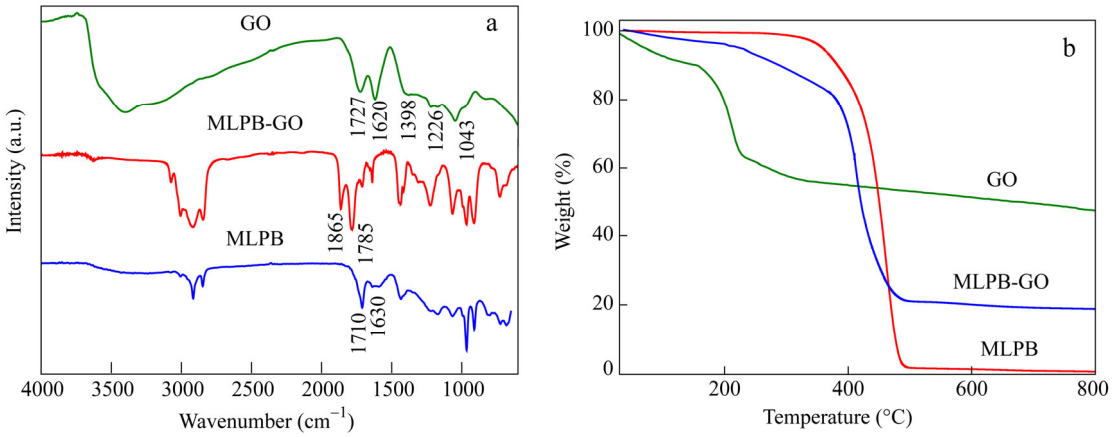

Fig. 1 FTIR spectra (a) and TGA curves (b) of GO, MLPB and MLPB-GO composites

XPS measurements were conducted to investigate the chemical compositions of GO and MLPB-GO. As shown in Fig. 2(a), the deconvoluted C 1s curve of GO contains four types of carbon atoms, namely sp^2 hybridized carbon (284.5 eV), the C atom in the C—O bond (286.7 eV), the carbonyl C (287.8 eV) and the carboxylate C in O—C=O (288.7 eV)[28, 29]. As for MLPB-GO (Fig. 2b), the peak intensity of C—O bond is much weaker than that of GO, whereas the peak intensity of O—C=O is much stronger than that in GO. These results strongly reveal that the MLPB is effectively grafted onto the GO.

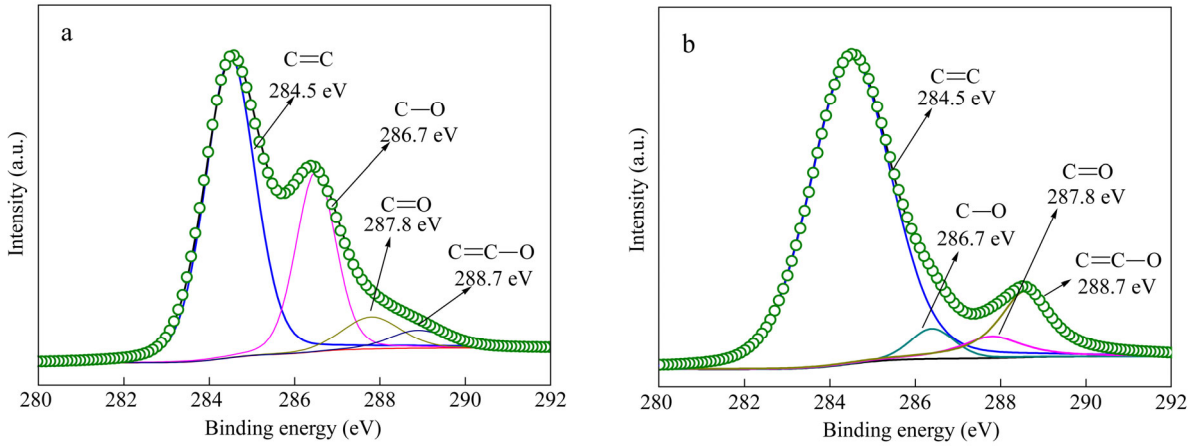

Fig. 2 XPS C 1s spectra of GO (a) and MLPB-GO (b)

The morphology of the MLPB-GO has been studied by AFM measurements. In Fig. 3(a), it can be seen that the GO sheets have a lateral dimension ranging from a few hundred nanometers to several micrometers and a characteristic thickness ranging from 0.9 nm to 1.0 nm, which is in accordance with other reports[30, 31]. After functionalization, the thickness of MLPB-GO (3.2 nm) is much higher than that of GO. The increase in the thickness can be rationalized in terms of the graft of the MLPB onto GO sheets.

FESEM was further used to investigate the evolution of morphology and structure of the GO sheets before and after grafting functionalization. As shown in Figs. 4(a) and 4(b), the wrinkled and tangled GO sheets clearly exhibit. And the GO sheets are highly transparent, illustrating that the GO sheets are quite thin. As for MLPB-GO (Figs. 4c and 4d), the GO sheets are wrapped or covered by a very thick MLPB layer. Such observations strongly suggest that the surfaces of GO sheets were successfully grafted by MLPB.

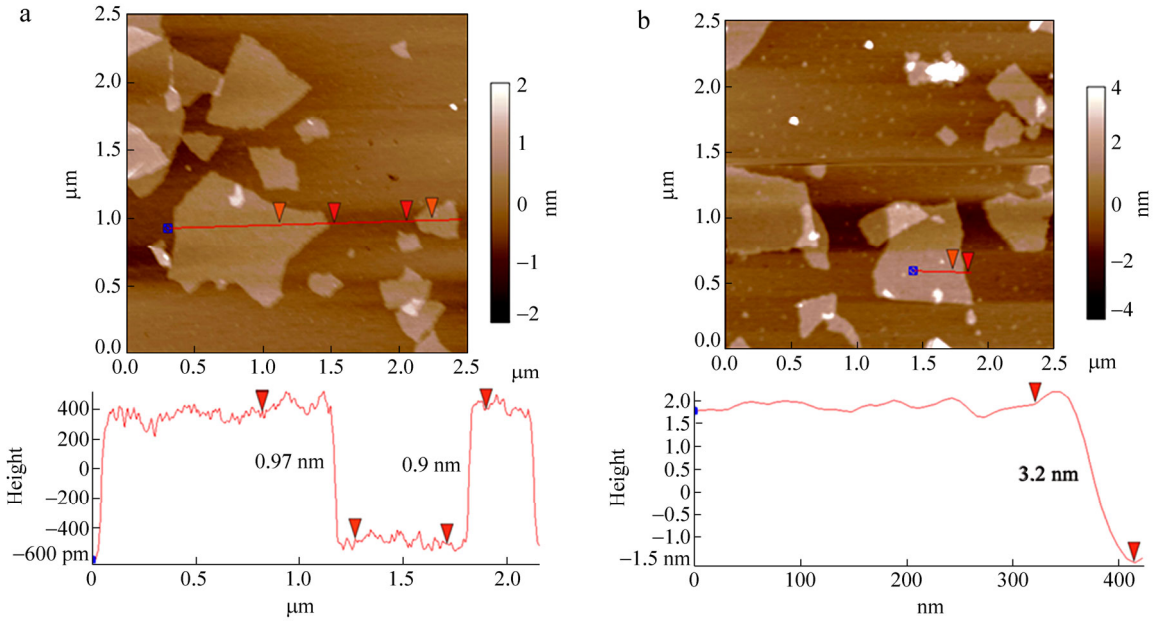

Fig. 3 AFM images with high profiles of GO (a) and MLPB-GO (b)

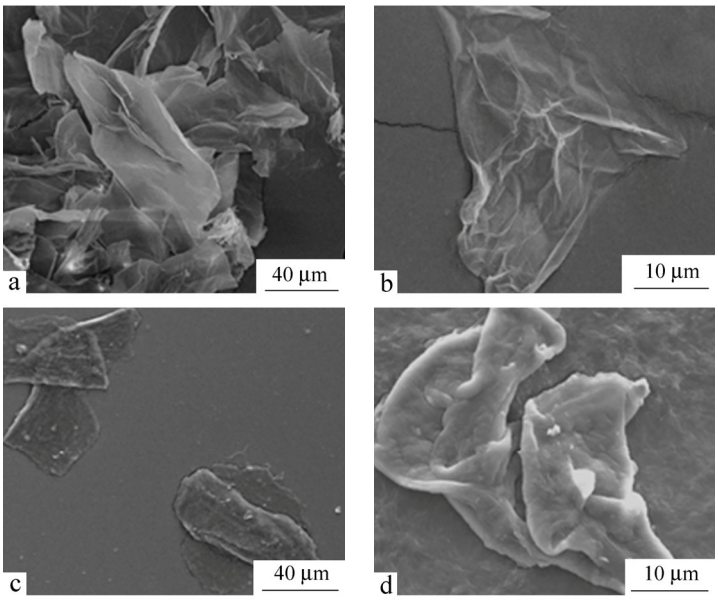

Fig. 4 FESEM images of GO (a, b) and MLPB-GO (c, d)

Structures and Performance of NR/MLPB-GO Composites

It is well known that MLPB is an unsaturated flexible macromolecule. Due to the graft of MLPB onto the GO sheets, it makes MLPB-GO especially promising in the fabrication of rubber/GO composites. Accordingly, we prepared a series of NR composites with different MLPB-GO contents to investigate the reinforcement efficiency of MLPB-GO toward NR.

FESEM and HRTEM were employed to evaluate the dispersion state of GO sheets in the NR composites. As presented in Fig. 5, the FESEM images of cryogenically fractured surfaces for neat NR, NR/GO-2.12 and NR/MLPB-GO-2.12 composites are compared. For all cases, the observed white points are the rubber additives, ascribed to the excessive ZnO which do not participate in the curing reaction, which is consistent with the results

of XRD analysis in Fig. 7. And it is seen that the surface of neat NR displays a generally smooth morphology (Figs. 5a and 5b), whereas NR/GO-2.12 and NR/MLPB-GO-2.12 composites exhibit more rough fractured surfaces with convex structure, shown in Figs. 5(c), 5(d), 5(e) and 5(f). As reported previously for rubber/grapheme composites[32, 33], these convex structures are mainly derived from the introduced GO sheets entrapped by rubber chains. However, as for NR/GO-2.12 composite, some aggregates are observed (Figs. 5c and 5d), the GO sheets or GO aggregates are pulled out from the matrix, and the cavity in the NR-GO interface is clearly observed, showing a poor adhesion between these two components in the NR/GO composites. By contrast, it displays no aggregates for NR/MLPB-GO-2.12 composite, shown in Figs. 5(c) and 5(d). It is noted that the GO sheets were embedding in the matrix, and the GO sheets are not pulled out after the fracture and the NR-GO interface is blurry. All of these observations reveal the strong adhesion between GO and NR matrix. This is because the GO sheets are grafted with thick MLPB layers, and MLPB with high unsaturation can facilitate the graft-polymerization with NR during the curing process, forming the complex crosslinked network. Thus, the poly-(MLPB) serves as "bridge" which is attached with GO on one end and linked to rubber chains on the other end, providing the strong interfacial interaction between GO and rubber matrix.

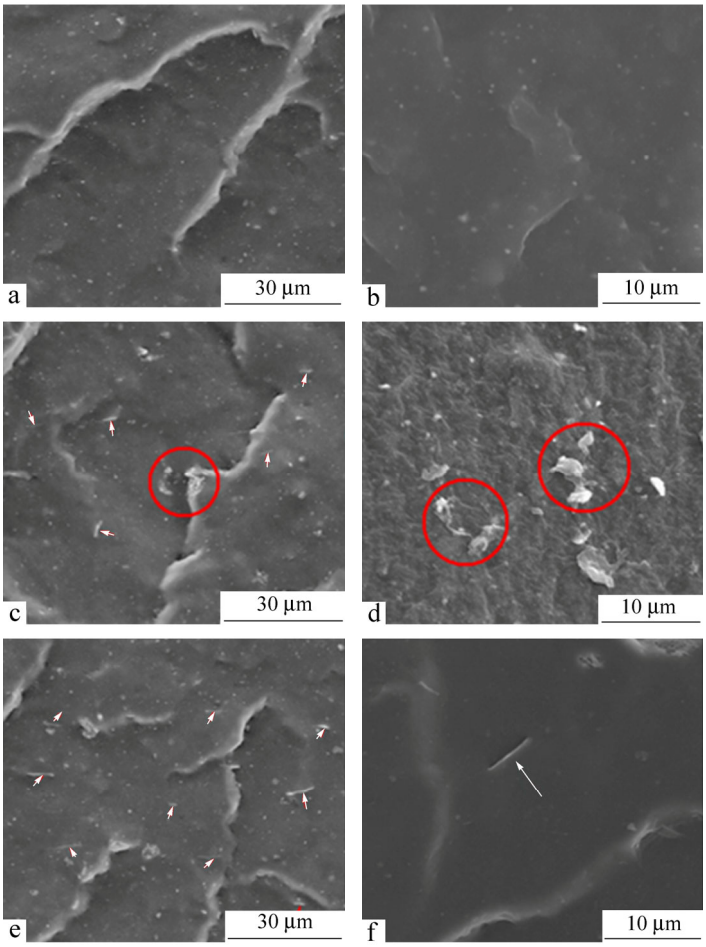

Fig. 5 FESEM images of neat NR (a, b), NR/GO-2.12 (c, d) and NR/MLPB-GO-2.12 composite (e, f)
White arrows indicate the GO sheets embedded in the matrix and circles present the aggregates of GO sheets.

Furthermore, HRTEM was also used to directly analyze the dispersed state of MLPB-GO sheets in the matrix. Obviously, for NR/GO-2.12 composite, the apparent stacking of GO sheets exhibits in Fig. 6(a). This may be attributed to the decreased distance between GO sheets in NR latex at high GO loading, so that the aggregation of GO sheets is formed due to the faster aggregation rate of GO sheets than latex articles when latex coagulation is occurred[34]. However, as for NR/MLPB-GO-2.12 composite, it can be seen that almost all of the GO sheets are dispersed in the matrix as single layers (Fig. 6b). No aggregates are observed in the view, which also may be due to the poly-(MLPB) grafted onto the GO sheets, as the effective barriers, inhibit the aggregation of GO.

The dispersion of the GO sheets in the composites was further characterized by XRD. Figure 7 shows the XRD patterns of GO, neat NR, NR/GO and NR/MLPB-GO composites. In the patterns of GO, the (001) diffraction peak around 10.2° (interlayer spacing of 0.87 nm) characterizing GO stacking is found. For neat NR, a broad diffraction peak is clearly observed, revealing a noncrystalline structure of neat NR. It is clearly observed that the XRD patterns of all NR/GO and NR/MLPB-GO composites are similar to that of neat NR, all without the diffraction peak for GO, which indicates that GO and MLPB-GO have been well-dispersed in the NR matrix. The other diffraction peaks are observed for all composites, ascribed to the excessive ZnO which do not participate in the curing reaction.

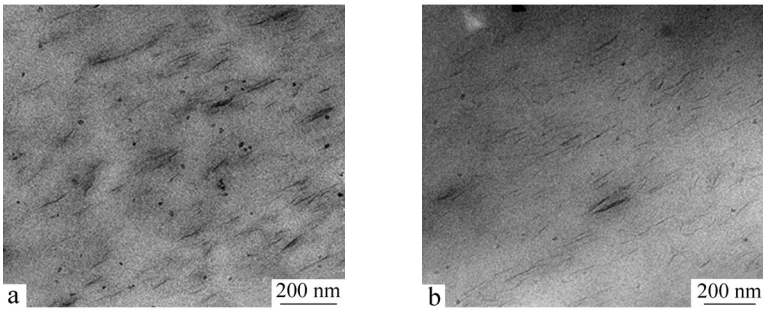

Fig. 6 HRTEM images of NR/GO-2.12 composite (a) and NR/MLPB-GO-2.12 composite (b)

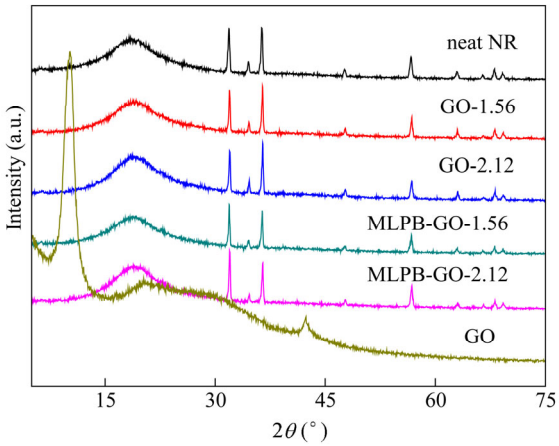

Fig. 7 XRD patterns of GO, neat NR, NR/GO and NR/MLPB-GO composites

Mechanical Performance of NR/MLPB-GO Composites

The mechanical performance of NR/MLPB-GO composites is enhanced by the uniform dispersion of GO in the NR matrix and the strong interfacial interaction between GO and NR. The effect of MLPB-GO loading on the mechanical properties of NR composites is illustrated in Fig. 8(a) and Table 1. Compared with neat NR, the mechanical properties of NR/MLPB-GO composites dramatically improved with the increasing MLPB-GO loading. For example, the tensile strength, modulus at 300% strain and tear strength of NR/MLPB-GO-2.12

composites are significantly enhanced to 22.9 MPa, 2.3 MPa and 35.7 kN/m, increasing by 40.5%, 109.1% and 85.0%, respectively. It is expected to see that the NR/MLPB-GO composites exhibit superior mechanical properties to those of NR/GO composites. The tensile strength of NR/MLPB-GO-1.56 composite is about the same as that of NR/GO-2.12. And with increasing the MLPB-GO loading to 2.12 phr, the tensile strength, modulus at 300% strain and tear strength of composite is dramatically enhanced to 22.9 MPa, 2.3 MPa and 35.7 kN/m, increasing by 13.4%, 27.8% and 34.7% as compared with NR/GO-2.12 composite, respectively. However, the elongation at break of NR/GO composites decreases with increasing the GO loading, which is due to that high GO loading provides more chemical and physical crosslink points, restricting the movement of rubber chains[35]. For NR/MLPB-GO composites, the elongation at break follows a similar trend to that of NR/GO composites. This is because that GO sheets produce the physical crosslink points, and MLPB grafted onto the GO sheets can take the graft-polymerization to form a complex crosslink network during vulcanization. As a result, the mobility of the rubber chain segments can be greatly restricted. The improvement in mechanical properties will be further validated by swelling measurements in the following discussion.

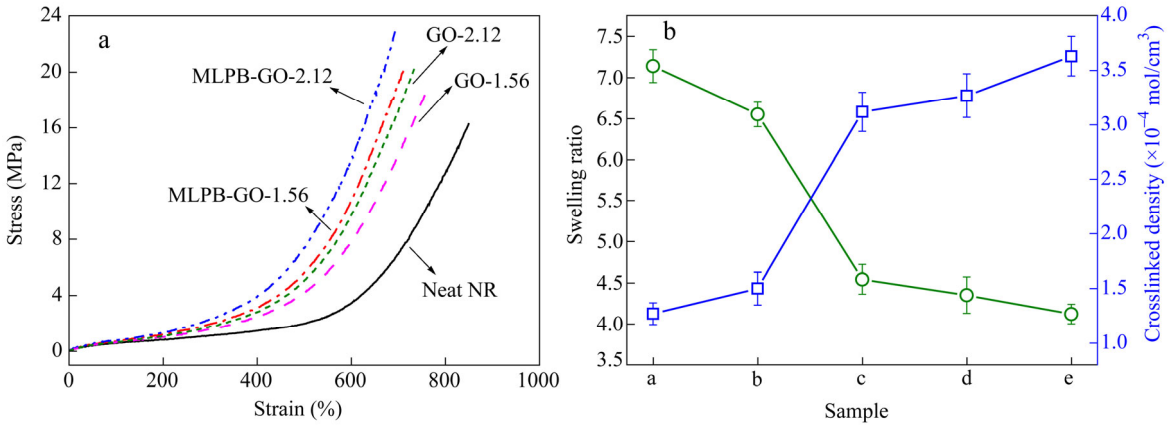

Fig. 8 Stress-strain curves (a), and swelling ratio and crosslink density (b) of NR composites (a: neat NR, b: NR/GO-1.56, c: NR/GO-2.12, d: NR/MLPB-GO-1.56 and e: NR/MLPB-GO-2.12)

Table 1. Mechanical properties of neat NR, NR/GO and NR/MLPB-GO composites

Sample	Tensile strength (MPa)	Elongation at break (%)	Modulus at 300% strain (MPa)	Tear strength (kN/m)
neat NR	16.3 ± 0.45	849 ± 45	1.1 ± 0.12	19.3 ± 0.60
GO-1.56	18.7 ± 0.56	760 ± 38	1.6 ± 0.19	24.3 ± 0.85
GO-2.12	20.2 ± 0.68	733 ± 30	1.8 ± 0.22	26.5 ± 0.90
MLPB-GO-1.56	20.5 ± 0.71	714 ± 27	2.0 ± 0.26	30.3 ± 0.98
MLPB-GO-2.12	22.9 ± 0.82	693 ± 24	2.3 ± 0.30	35.7 ± 1.10

It is well known that the mechanical properties of composites are closely related to the crosslink density of composites. The crosslink density and swelling ratio of NR/MLPB-GO composites were calculated, and the results are shown in Fig. 8(b). Apparently, with increasing GO loading, the crosslink density increases significantly, whereas the swelling ratio decreases. For example, compared to neat NR, the crosslink density of the NR/GO-2.12 composite increases by 146%, while the swelling ratio of the composite decreases by 36%. It is believed that the curled GO sheets with a large scale can be entangled with rubber chains, producing physical crosslink points, leading to the great improvement of crosslink density. Moreover, using sulfur as a curing agent, the synthesized GO bears −OH and −COOH groups, which were converted into thiol (−SH), thioester (−CSOR) and dithiocarboxylic ester (−CSSR) groups upon reaction with sulfur. The polysulfides species reacted with the unsaturated sites on the rubber chains and form polysulfidic crosslinks[35, 36], greatly increased the crosslinking density of the composites. Therefore, NR/GO-2.12 composites showed much high crosslinking density. Additionally, it is observed that the crosslink densities of NR/MLPB-GO composites are much higher

than those of NR/GO composites. When adding 1.56 phr MLPB-GO, the crosslink density of NR/MLPB-GO-1.56 composite is a litter higher than that of NR/GO-2.12 composite. With increasing the MLPB-GO loading to 2.12 phr, the NR/MLPB-GO-2.12 composite increases by 16.3% over that of the NR/GO-2.12 composite. Noteworthily, after the grafting of MLPB onto GO, the amount of —OH groups on GO sheets significantly decreases, which greatly affects the amount of the formed polysulfidic crosslinks. Therefore, these results reveal that MLPB has a great effect on maturing the crosslinked network. During the vulcanization, the unsaturated MLPB molecules can provide more active crosslinking points to constitute the complex rubber network.

DMA is used to evaluate the effects of MLPB-GO on dynamic response of NR composites. Figure 9(a) shows the storage modulus curves of neat NR, NR/GO and NR/MLPB-GO composites as a function of temperature at 1 Hz. The storage modulus of NR composite is improved significantly with the incorporation of GO and MLPB-GO. And it is seen that the storage modulus of NR/MLPB-GO composites is much higher than that of neat NR and NR/GO composites. For example, the storage modulus of MR/MLPB-GO-2.12 composite is 84% higher than that of neat NR. This indicates that the elastic response of NR/MLPB-GO composites towards deformation is superior to that of neat NR and NR/GO composites. Moreover, the temperature dependence of the mechanical loss factor (tanδ) is plotted in Fig. 9(b). One peak located at about −60 °C is observed in all curves, which corresponds to the glass transition temperature (T_g). In comparison with neat NR, T_g of the NR/GO composites is obviously shifted to a higher temperature with increasing the GO loading. This is due to the increasing ratio of GO sheets can provide more crosslinked points, which restricts the motion of the rubber molecular chains. Also, compared with NR/GO composites, T_g of NR composites shifts to higher temperature with the incorporation of MLPB-GO, which reflects the more complex crosslinked network and demonstrates the stronger interfacial interaction between GO and NR. Briefly, T_g of NR/MLPB-GO-2.12 composite is 2.0 K higher than that of NR/GO-2.12 composite, and 2.9 K higher than that of neat NR. Therefore, we believe that the good dispersion of GO and the strong interface interaction in the composites are responsible for such unprecedented reinforcing efficiency of MLPB-GO towards NR.

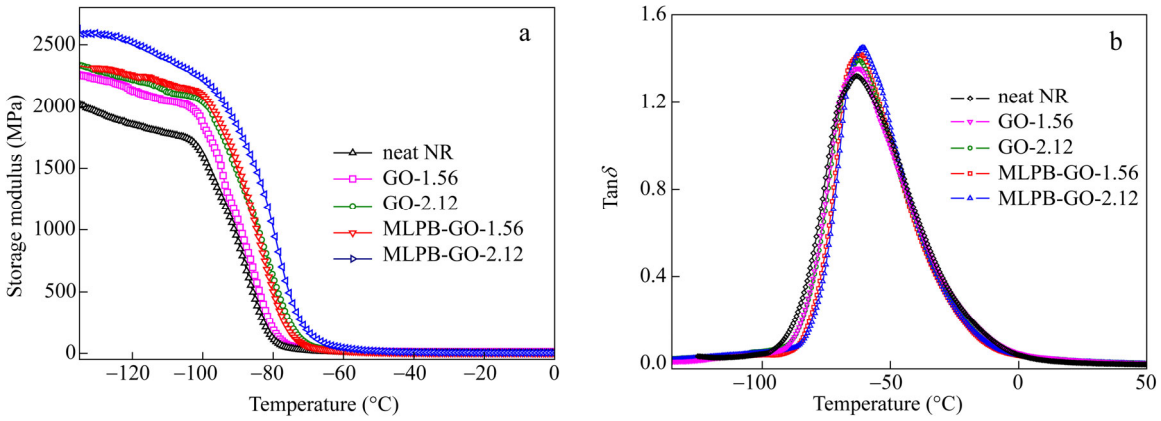

Fig. 9 Storage modulus (a) and tanδ (b) of NR composites as a function of temperature

CONCLUSIONS

In this work, the maleic anhydride-grafted liquid polybutadiene functionalized graphene oxide sheets (MLPB-GO) were prepared by grafting MLPB onto GO sheets. The obtained MLPB-GO can be well dispersed in the NR matrix, which is confirmed by FESEM and HRTEM observations. Compared with neat NR, the fabricated NR/MLPB-GO composites show enhanced mechanical properties, such as the improved tensile strength, modulus at 300% strain, tear strength, storage modulus, and higher T_g. And the mechanical properties of NR/MLPB-GO composites are obviously superior to those of NR/GO composites and neat NR. The strong interface interaction and the good dispersion of MLPB-GO in the composites are responsible for these high performances.

REFERENCES

1 Arroyo, M., López-Manchado, M.A. and Herrero, B., Polymer, 2003, 44(8): 2447
2 Bitinis, N., Hernandez, M., Verdejo, R., Kenny, J.M. and Lopez-Manchado, M.A., Adv. Mater., 2011, 23(44): 5229
3 Yan, L., Zheng, Y.B., Zhao, F., Li, S., Gao, X., Xu, B., Weiss, P.S. and Zhao, Y., Chem. Soc. Rev., 2012, 41(1): 97
4 Wei, W. and Qu, X., Small, 2012, 8(14): 2138
5 Scharfenberg, S., Rocklin, D.Z., Chialvo, C., Weaver, R.L., Goldbart, P.M. and Mason, N., Appl. Phys. Lett., 2011, 98(9): 091908
6 Wang, J.Y., Jia, H.B., Tang, Y.Y., Ji, D.D., Sun, Y., Gong, X.D. and Ding, L.F., J. Mater. Sci., 2013, 48(4): 1571
7 Kim, H.M., Lee, J.K. and Lee, H.S., Thin Solid Films, 2011, 519(22): 7766
8 Yadav, M., Rhee, K.Y., Jung, I.H. and Park, S.J., Cellulose, 2013, 20(2): 687
9 Bai, X., Wan, C., Zhang, Y. and Zhai, Y., Carbon, 2011, 49(5): 1608
10 Wu, J., Huang, G., Li, H., Wu, S., Liu, Y. and Zheng, J., Polymer, 2013, 54(7): 1930
11 Huang, Y.J., Qin, Y.W., Zhou, Y., Niu, H., Yu, Z.Z. and Dong, J.Y., Chem. Mater., 2010, 22(13): 4096
12 Hu, H.T., Wang, X.B., Wang, J.C.,Wan, L., Liu, F.M., Zheng, H., Chen, R. and Xu, C.H., Chem. Phys. Lett., 2010, 484(4−6): 247
13 Wang, X., Hu, Y.A., Song, L., Yang, H.Y., Xing, W.Y. and Lu, H.D., J. Mater. Chem., 2011, 21(12): 4222
14 Lin, Y., Jin, J. and Song, M., J. Mater. Chem., 2011, 21(10): 3455
15 He, H.K. and Gao, C., Chem. Mater., 2010, 22(17): 5054
16 Wu, J.R., Huang, G.S., Li, H., Wu, S.D., Liu, Y.F. and Zheng, J., Polymer, 2013, 54(7): 1930
17 Yang, H., Li, F., Shan, C., Han, D., Zhang, Q., Niu, L. and Ivaska, A., J. Mater. Chem., 2009, 19(26): 4632
18 Hsiao, M.C., Liao, S.H., Yen, M.Y., Liu, P., Pu, N.W., Wang, C.A. and Ma, C.C., ACS Appl. Mater. Inter., 2010, 2(11): 3092
19 Shen, J., Shi, M., Ma, H.,Yan, B., Li, N., Hu, Y. and Ye, M., J. Colloid Interf. Sci., 2010, 352(2): 366
20 Pham, T.A., Kumar, N.A. and Jeong, Y.T., Syn. Met., 2010, 160: 2028
21 Avinash, M.B., Subrahmanyam, K.S., Sundarayya, Y. and Govindaraju, T., Nanoscale, 2010, 2: 1762
22 Stankovich, S., Piner, R.D., Nguyen, S.T. and Ruoff, R.S., Carbon, 2006, 44: 3342
23 Yang, H.H., Cao, X.Y., Ma, Y.M., An, J.J., Ke, Y.C., Liu, X.M. and Wang, F.S., Polym. Eng. Sci., 2012, 52(3): 481
24 Shibulal, G.S. and Naskar, K., J. Appl. Polym. Sci., 2013, 130(3): 2205
25 Li, H.B., Lu, T., Pan, L.K., Zhang, Y.P. and Sun, Z., J. Mater. Chem., 2009, 19(37): 6773
26 Kang, H.L., Zuo, K.H., Wang, Z., Zhang, L.Q., Liu, L. and Guo, B.C., Compos. Sci. Technol., 2014, 92: 1
27 Stankovich, S., Dikin, D.A., Piner, R.D., Kohlhaas, K.A., Kleinhammes, A., Jia, Y.Y., Wu, Y., Nguyen, S.T. and Ruoff, R.S., Carbon, 2007, 45(7): 1558
28 Yang, H., Shan, C., Li, F., Han, D., Zhang, Q. and Niu, L., Chem. Commun., 2009, 26: 3880
29 Wang, Y., Shi, Z. and Yin, J., ACS Appl. Mater. Inter., 2011, 3(4): 1127
30 Liao, R.J., Tang, Z.G., Lei, Y.D. and Guo, B.C., J. Phys. Chem. C, 2011, 115(42): 20740
31 Zeng, C., Tang, Z., Guo, B. and Zhang, L., Phys. Chem. Chem. Phys., 2012, 14(28): 9838
32 Tang, Z.H., Wu, X.H., Guo, B.C., Zhang, L.Q. and Jia, D.M., J. Mater. Chem., 2012, 22(15): 7492
33 Wang, J., Jia, H., Tang, Y., Ji, D., Sun, Y., Gong, X. and Ding, L., J. Mater. Sci., 2013, 48(4): 1571
34 Potts, J.R., Shankar, O., Du, L. and Ruoff, R.S., Macromolecules, 2012, 45(15): 6045
35 Wu, J.R., Xing, W., Huang, G.S., Li, H., Tang, M.Z., Wu, S.D. and Liu, Y.F., Polymer, 2013, 54(13): 3314
36 Tang, M.Z., Xing, W., Wu, J.R., Huang, G.S., Li, H. and Wu, S.D., Chinese J. Polym. Sci., 2014, 32(5): 658